

**Electronic Supplementary Information (ESI)**

## **Geometric control of multi-resonance backbone DABNA for narrowband deep-blue electroluminescence**

Hao Wu,<sup>a</sup> Yi-Zhong Shi,<sup>\*b</sup> Mo-Yuan Li,<sup>a</sup> Xiao-Chun Fan,<sup>a</sup> Hui Wang,<sup>a</sup> Tong-Yuan Zhang,<sup>a</sup> Jia Yu,<sup>\*a</sup> Kai Wang,<sup>\*ac</sup>, and Xiao-Hong Zhang<sup>\*ad</sup>

<sup>a</sup> Institute of Functional Nano & Soft Materials (FUNSOM), Soochow University, 199 Ren'ai Road, Suzhou, 215123, Jiangsu, PR China

<sup>b</sup> School of Materials Science and Engineering, Suzhou University of Science and Technology, Suzhou, 215009, PR China

<sup>c</sup> Jiangsu Key Laboratory for Carbon-Based Functional Materials & Devices, Soochow University, Suzhou, 215123, Jiangsu, PR China

<sup>d</sup> Jiangsu Key Laboratory of Advanced Negative Carbon Technologies, Soochow University, Suzhou, 215123, Jiangsu, PR China

### **Corresponding Author**

yzshi@mail.usts.edu.cn, yujia199019@suda.edu.cn, wkai@suda.edu.cn, xiaohong\_zhang@suda.edu.cn

## General Information

**Material.** All reagents and solvents were purchased from Xi'an Yizhichen Biotechnology Co., LTD and used without further purification unless specially noted. The main synthesis was performed using standard Schlenk techniques under a nitrogen atmosphere, and the target compound was further purified by sublimation.  $^1\text{H}$  and  $^{13}\text{C}$  NMR spectra were measured on a Bruker 600/400 MHz spectrometer with tetramethylsilane (TMS) as the internal standard. Mass analyses were recorded by an Autoflex MALDI-TOF mass spectrometer.

**Single Crystal Structure.** Diffraction data were collected on a Rigaku R-AXIS-RAPID diffractometer using  $\omega$ -scan mode with graphite-monochromator MoK $\alpha$  radiation. The structure determination was solved with direct methods using the SHELXTL programs and refined with full-matrix least squares on F2. All crystallographic information in CIF format has been deposited at the Cambridge Crystallographic Center (CCDC) under deposition number 2364352 for c-DABNA via [www.ccdc.cam.ac.uk/data\\_request/cif](http://www.ccdc.cam.ac.uk/data_request/cif).

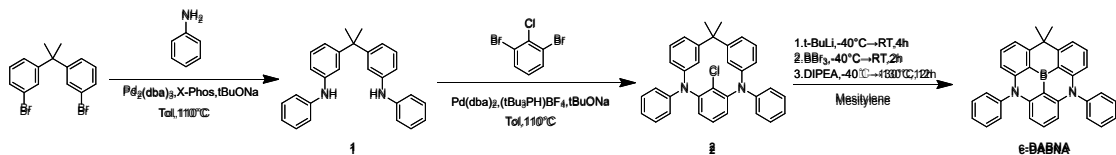
**Theoretical calculation.** The density functional theory (DFT) and time-dependent DFT (TD-DFT) calculations were first performed at the PBE0/6-31G(d) basis set in the Gaussian 16 program package. All calculations were performed in the gas phase. The molecular structure, frontier molecular orbital, and electron distribution models were rendered by Multiwfn and VMD. (1.9.3)<sup>1,2</sup>.

**Electrochemical and thermal measurement.** Cyclic voltammetry (CV) curves were recorded on a CHI660e electrochemistry station in oxygen-free N,N-Dimethylformamide (DMF) solution with tetrabutylammonium hexafluorophosphate ( $\text{Bu}_4\text{NPF}_6$ ) at a scan rate of 0.1 V s $^{-1}$ . Thermogravimetric analysis (TGA) curves were obtained on a Perkin Elmer at a heating rate of 10 °C min $^{-1}$  under nitrogen. The temperature of 5% weight loss was defined as the decomposition temperature ( $T_d$ ). Differential scanning calorimetry (DSC) curves were obtained on a TA DSC 2010 unit at a heating rate of 10 °C·min $^{-1}$  from 25 to 280 °C under nitrogen.

**Photophysical measurement.** UV–Vis absorption and photoluminescence (PL) spectra were recorded by using a Hitachi ultraviolet–visible (UV–Vis) spectrophotometer U-3010 and a Hitachi fluorescence spectrometer F-4600, respectively. PL quantum efficiency (PLQY) was measured via the absolute PL quantum yield measurement system (C11347-01, Hamamatsu Photonics) under the flow of nitrogen gas with an excitation wavelength of 300 nm. Transient decay measurements were carried out with an Edinburgh fluorescence spectrometer (FLS920).

**Device Characterization.** OLEDs were fabricated on indium-tin oxide (ITO)-coated transparent glass substrates with multiple layers. The ITO glass substrates have a thickness of ca. 100 nm and a sheet resistance of ca. 30 Ω per square and were cleaned with optical detergent, deionized water, acetone, and isopropanol successively and then dried in an oven. For vacuum-evaporation OLEDs, the ITO substrates were exposed to UV ozone for 15 minutes at first. All the organic materials were thermally evaporated at a rate of 1 Å s $^{-1}$  under a vacuum of ca. 10 $^{-5}$  Torr. Finally, LiF and Al were successively deposited at rates of 0.1 Å s $^{-1}$  and 5 Å s $^{-1}$ , respectively. Four identical OLED devices were formed on each of the substrates, and the emission area was 0.10 cm $^2$  for each device. The electrical characteristics of the devices were measured with a Keithley 2400 source meter. The electroluminescence (EL) spectra and luminance of the devices were obtained on a PR655 spectrometer.

## Synthesis



**Scheme S1.** Synthetic routes for **c**-DABNA.

Synthesis of **1**: A mixture of 3,3'-(propane-2,2-diyl)bis(bromobenzene) (5.00 g, 14.1 mmol), aniline (2.79 g, 30.0 mmol),  $\text{Pd}_2(\text{dba})_3$  (732 mg, 0.8 mmol), X-Phos (732 mg, 1.6 mmol), tBuONa (4.32 g, 45.0 mmol) was added a solution of toluene, then the mixture was refluxed at 110 °C under  $\text{N}_2$  protection for 12 hours. After the reaction was cooled to room temperature, the mixture was extracted with dichloromethane and water three times to collect the organic layer. Then, the collection was dried with  $\text{Na}_2\text{SO}_4$  and concentrated with rotary evaporation. The residue was purified via column chromatography eluting to obtain a white solid (4.97 mg, yield: 94%).  $^1\text{H}$  NMR (400 MHz, Chloroform-*d*)  $\delta$  7.24 – 7.15 (m, 6H), 6.99 (d,  $J$  = 7.6 Hz, 4H), 6.93 (dd,  $J$  = 8.6, 1.5 Hz, 4H), 6.90 – 6.83 (m, 4H), 5.65 (s, 2H), 1.65 (s, 6H).  $^{13}\text{C}$  NMR (101 MHz,  $\text{CDCl}_3$ )  $\delta$  152.03, 143.38, 142.51, 129.30, 128.87, 120.61, 119.69, 117.32, 115.22, 77.35, 77.03, 76.71, 42.98, 30.57. MALDI-TOF MS (mass m/z): [M]<sup>+</sup> calcd for  $\text{C}_{27}\text{H}_{26}\text{N}_2$ , 378.52; found, 377.13.

Synthesis of **2**: A mixture of **1** (4.93 g, 13.0 mmol), 1,3-dibromo-2-chlorobenzene (3.6 g, 13.3 mmol),  $\text{Pd}(\text{dba})_2$  (747 mg, 1.3 mmol), ( $t\text{Bu}_3\text{PH}$ ) $\text{BF}_4^-$  (754 mg, 2.6 mmol), tBuONa (3.84 g, 40 mmol) was added a solution of toluene, then the mixture was refluxed at 110 °C under  $\text{N}_2$  protection for 12 hours. After the reaction was cooled to room temperature, the mixture was extracted with dichloromethane and water three times to collect the organic layer. Then, the collection was dried with  $\text{Na}_2\text{SO}_4$  and concentrated with rotary evaporation. The residue was purified via column chromatography eluting to obtain a white solid (2.60 g, yield: 41%).  $^1\text{H}$  NMR (400 MHz, Chloroform-*d*)  $\delta$  7.32 – 7.26 (m, 8H), 7.20 (dd,  $J$  = 8.4, 7.6 Hz, 1H), 7.04 (dd,  $J$  = 8.2, 4.5 Hz, 4H), 7.01 – 6.93 (m, 4H), 6.85 (t,  $J$  = 1.8 Hz, 2H), 6.80 (d,  $J$  = 7.4 Hz, 2H), 1.82 (s, 3H), 1.69 (s, 3H).  $^{13}\text{C}$  NMR (101 MHz,  $\text{CDCl}_3$ )  $\delta$  151.59, 149.53, 148.02, 145.43, 131.69, 129.22, 128.12, 128.06, 124.44, 122.83, 122.25, 120.86, 118.95, 117.00, 77.35, 77.03, 76.71, 41.56, 28.07, 23.49. MALDI-TOF MS (mass m/z): [M]<sup>+</sup> calcd for  $\text{C}_{33}\text{H}_{27}\text{N}_2\text{Cl}$ , 487.04; found, 486.23.

Synthesis of **c**-DABNA: The solution of *t*-butyllithium in pentane (5.0 mL, 1.3 M, 6.5 mmol) was added slowly to a solution of compound **2** (2.44 g, 5.0 mmol) in mesitylene (50 mL) at -40 °C under nitrogen atmosphere. After stirring at 60 °C for 2 h,  $\text{BBr}_3$  (0.8 mL, 8 mmol) was added dropwise at -40 °C. The mixture was slowly warmed to room temperature and stirred for additional 2 h. *N,N* diisopropylethylamine (DIPEA, 1.94 g, 15.0 mmol) was added at 0 °C and then the reaction mixture was heated to room temperature. After stirring at 160 °C for 12 h, the reaction mixture was cooled to room temperature. The resulted solution was extracted with dichloromethane/water, and the organic layer was concentrated in vacuum. The product was purified by column chromatography on silica gel to afford **c**-DABNA light-yellow solid (yield = 391 mg, 17%).  $^1\text{H}$  NMR (400 MHz, Chloroform-*d*)  $\delta$  7.71 – 7.65 (m, 4H), 7.60 – 7.55 (m, 2H), 7.51 – 7.46 (m, 2H), 7.45 – 7.38 (m, 6H), 7.29 – 7.24 (m, 1H), 6.50 (d,  $J$  = 8.3 Hz, 2H), 6.11 (d,  $J$  = 8.3 Hz, 2H), 1.85 (s, 6H).  $^{13}\text{C}$  NMR (101 MHz,  $\text{CDCl}_3$ )  $\delta$  155.12, 147.81, 146.35, 141.87, 133.02, 132.00, 130.94, 130.53, 128.51, 117.96, 112.63, 104.87, 77.36, 77.04, 76.72, 43.40, 34.95. MALDI-TOF MS (mass m/z): [M]<sup>+</sup> calcd for  $\text{C}_{33}\text{H}_{25}\text{BN}_2$ , 460.39; found, 460.26.

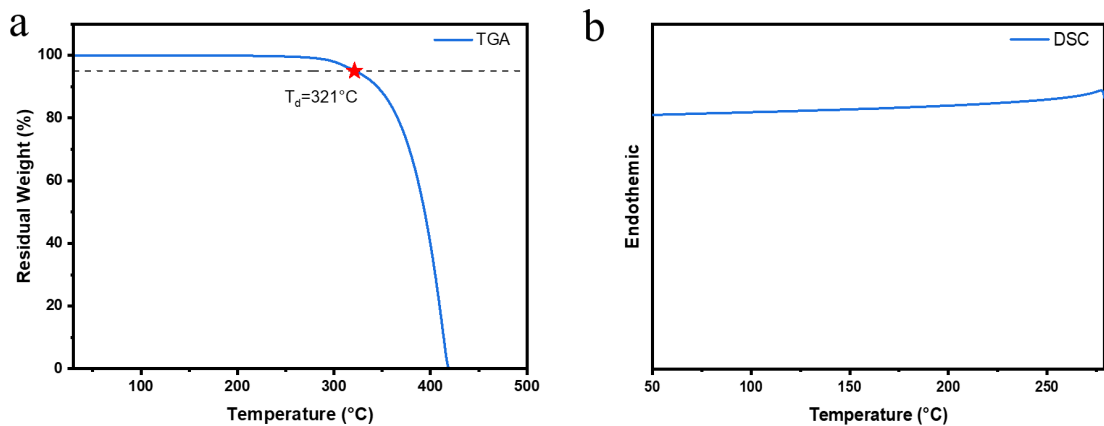


**Fig. S1.** a) Thermogravimetric analysis (TGA) and b) differential scanning calorimetry (DSC) curves of c-DABNA.

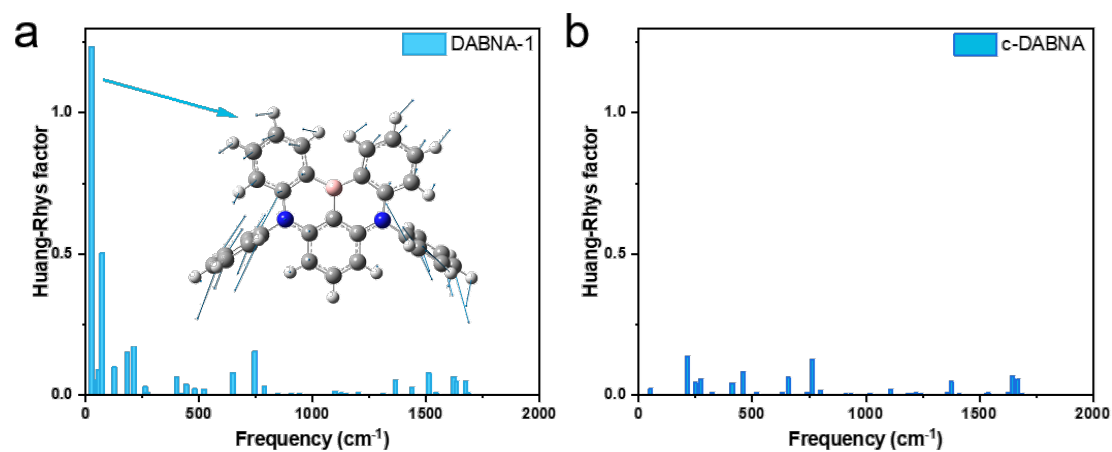


**Fig. S2.** HR factors for the  $\text{S}_1 \rightarrow \text{S}_0$  transition of a) DABNA-1 and b) c-DABNA.

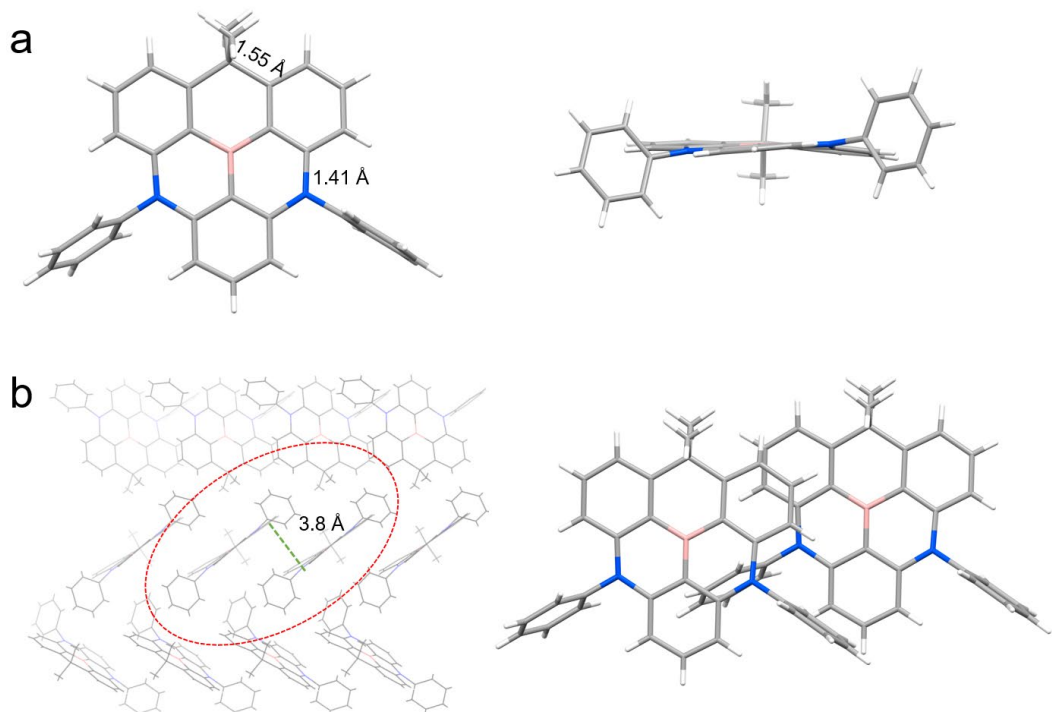


**Fig. S3.** (a) Molecular geometry and (b) packing diagram of c-DABNA in the single crystal.

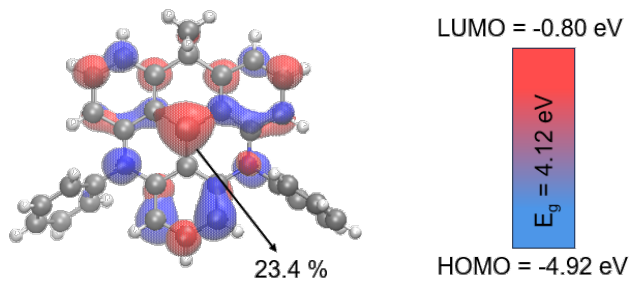


**Fig. S4.** Simulated FMOs of c-DABNA based on its single crystal geometry.

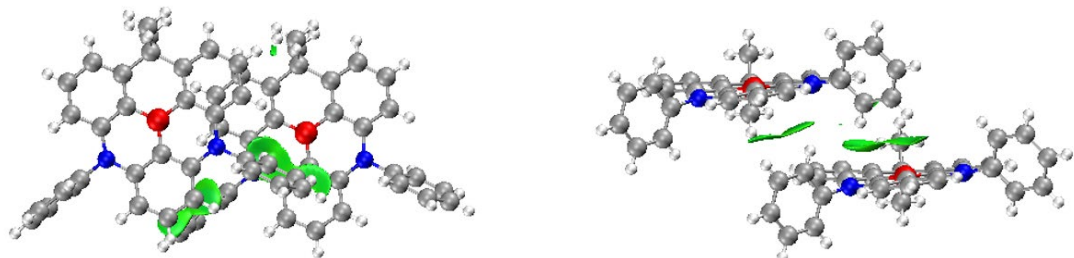


**Fig. S5.** Independent gradient model based on Hirshfeld partition (IGMH) isosurface of c-DABNA.

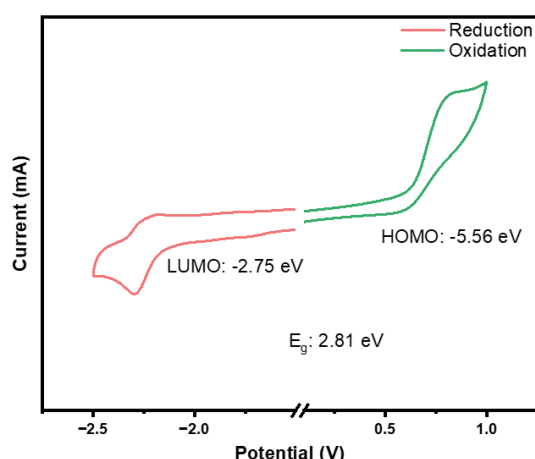


**Fig. S6.** Cyclic voltammetry (CV) curves of c-DABNA.

**Table S1.** Crystal data and structure refinements of c-DABNA.

Crystal Label	c-DABNA
Empirical formula	C <sub>33</sub> H <sub>25</sub> BN <sub>2</sub>
Formula weight	460.36
Temperature/K	170
Crystal system	orthorhombic
Space group	P2 <sub>1</sub> 2 <sub>1</sub> 2 <sub>1</sub>
a/Å	7.4246(4)
b/Å	11.3666(6)
c/Å	28.6369(17)
α/°	90
β/°	90
γ/°	90
Volume/Å <sup>3</sup>	2416.7(2)
Z	4
ρ <sub>calc</sub> g/cm <sup>3</sup>	1.265
μ/mm <sup>-1</sup>	0.073
F(000)	968.0
Crystal size/mm <sup>3</sup>	0.15 × 0.08 × 0.05
Radiation	MoKα ( $\lambda = 0.71073$ )
2θ range for data collection/°	3.856 to 52.748
Index ranges	-9 ≤ h ≤ 9, -14 ≤ k ≤ 14, -32 ≤ l ≤ 35

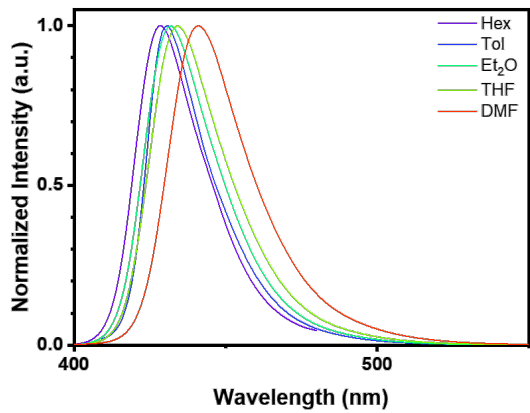


**Fig. S7.** The emission spectra of c-DABNA in solvents with different polarities.

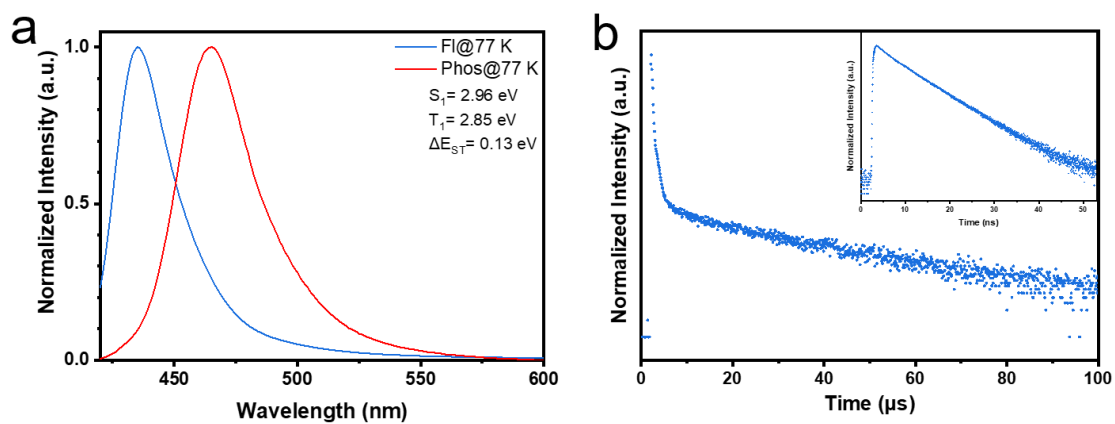


**Fig. S8.** a) The fluorescence and phosphorescence spectrum at 77 K, and b) transient PL decay curves of c-DABNA doped in mCP film with 1 wt % at room temperature.

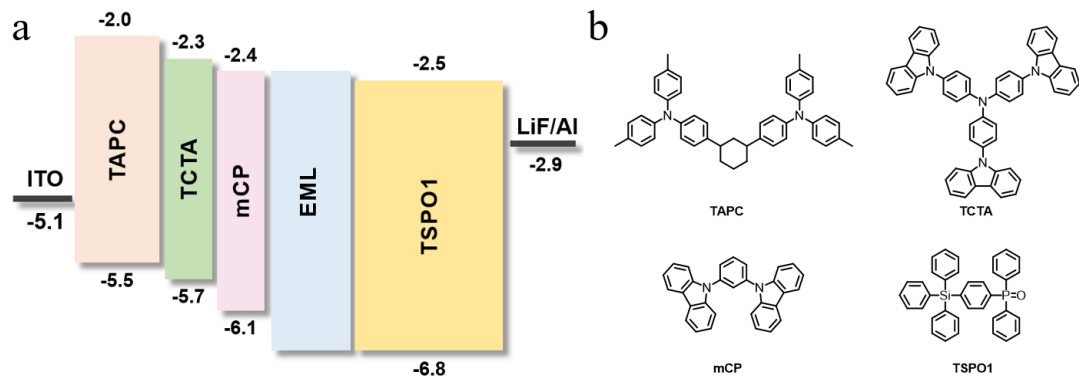


**Fig. S9.** The energy level diagram of the a) OLEDs and b) the molecular structures of the applied materials.

**Table S2.** Summary of the EL data of the c-DABNA-based devices.

Device	V <sub>on</sub> (V)	λ <sub>Max</sub> (nm)	FWHM (nm)	CE <sub>Max</sub> (cd·A <sup>-1</sup> )	PE <sub>Max</sub> (lm·W <sup>-1</sup> )	EQE <sub>Max</sub> (%)	CIE (x, y)	Blue Index
Binary	3.8	433	26	9.8	8.0	17.1	(0.156, 0.033)	297
Ternary	3.8	433	31	20.3	13.8	28.2	(0.156, 0.055)	369

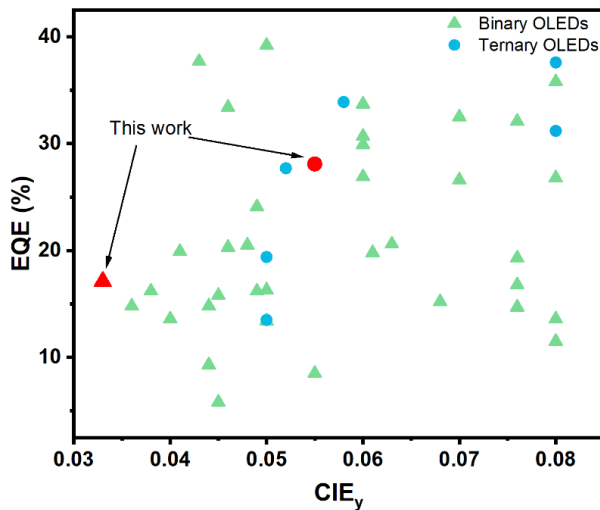


**Fig. S10.** Summary of the CIE<sub>y</sub> versus EQE<sub>Max</sub> of OLEDs based on reported MR materials with CIE<sub>y</sub> coordinates ≤ 0.08.

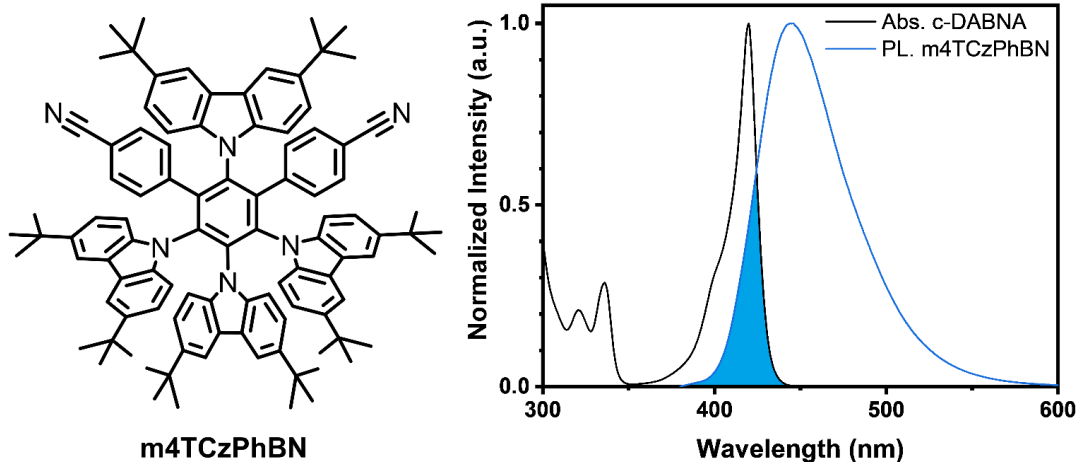
**Table S3.** Reported deep-blue MR OLEDs with CIE<sub>y</sub> coordinate ≤ 0.08 vs this work.

Emitter	λ <sub>EL</sub> (nm)	FWHM (nm)	EQE <sub>MAX</sub> (%)	CIE (x, y)	Ref.
c-DABNA	433	26	17.1	(0.156, 0.033)	This work
c-DABNA*	433	31	28.2	(0.156, 0.055)	
PAB	456	31	14.7	(0.145, 0.076)	
2tPAB	456	27	16.8	(0.145, 0.076)	3
3tPAB	460	26	19.3	(0.141, 0.076)	
IPrBN	457	22	20.6	(0.138, 0.063)	4
IPrBN-mCP	451	20	33.4	(0.146, 0.046)	
iPrAuBN	442	19	14.8	(0.154, 0.036)	5
[B-N]N2	441	20	20.3	(0.152, 0.046)	6
SAC2MN2B	448	25	19.8	(0.147, 0.061)	7

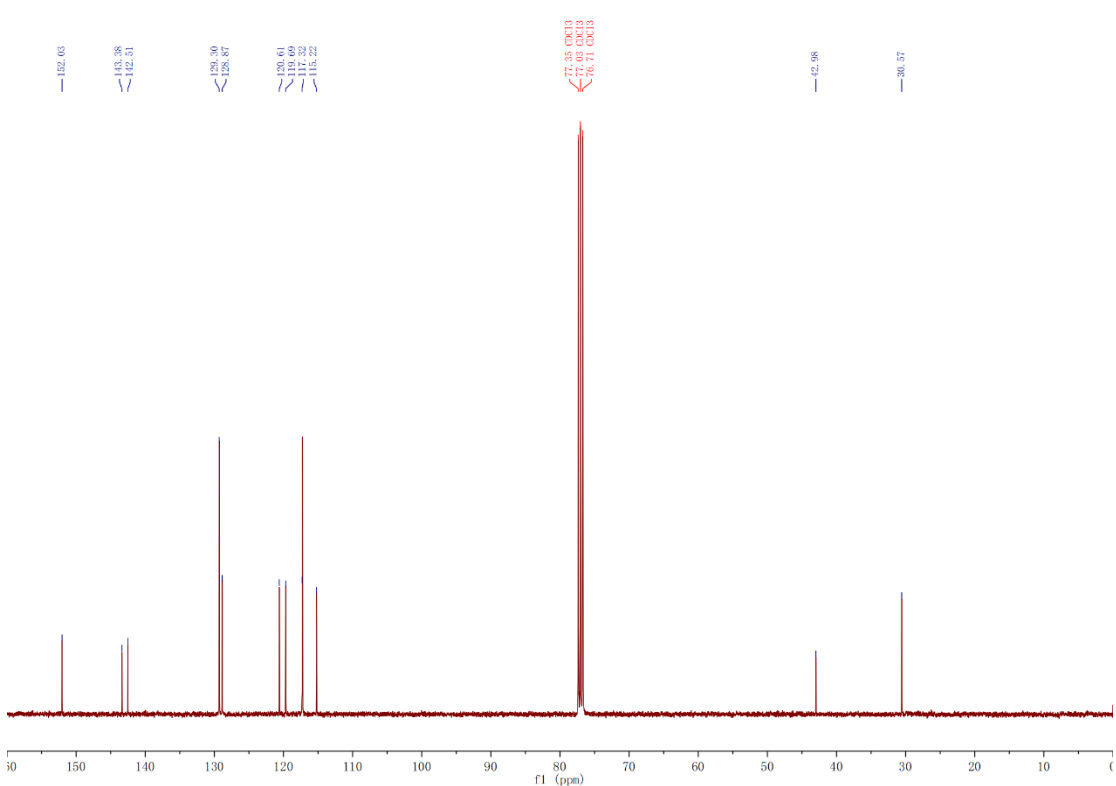
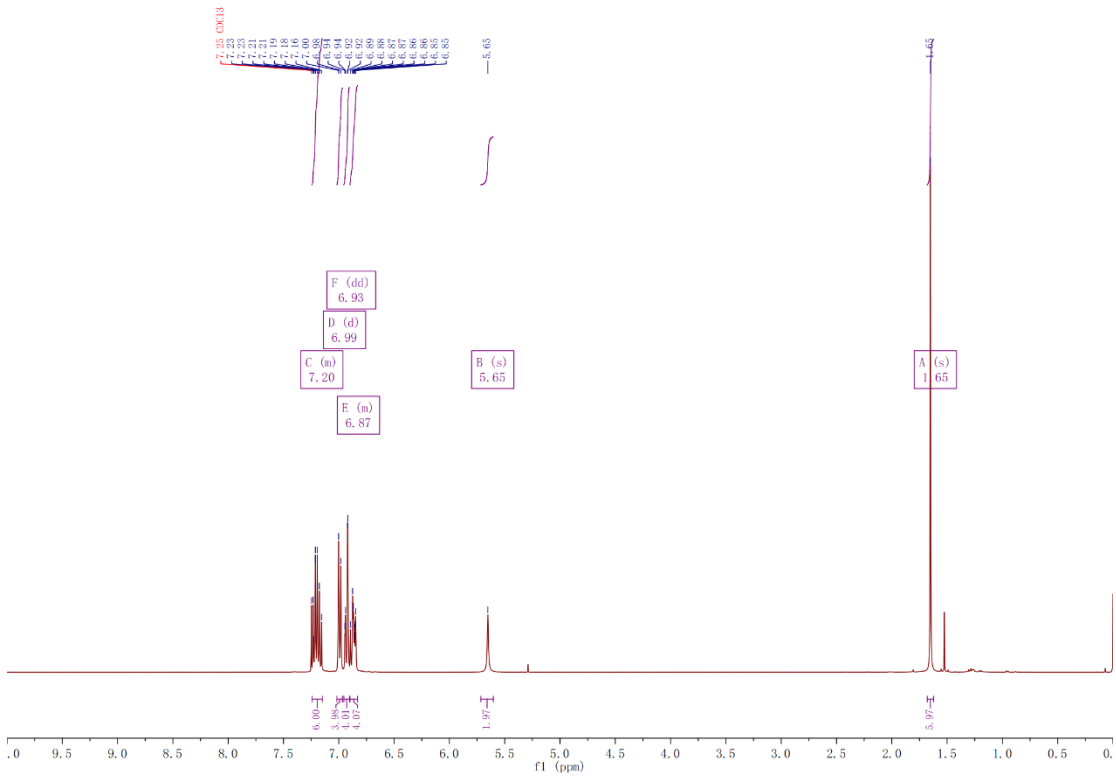
4F- <i>v</i> -DABNA	464	18	35.8	(0.13, 0.08)	8
4F- <i>m</i> - <i>v</i> -DABNA	461	18	33.7	(0.13, 0.06)	
<i>v</i> -DABNA-Az2	458	17	29.9	(0.140, 0.060)	9
C-BN	453	25	26.6	(0.14, 0.07)	10
B-O-dpa	443	32	16.3	(0.15, 0.05)	11
CzBNO	454	36	13.6	(0.14, 0.08)	12
CzBO	448	30	13.4	(0.15, 0.05)	13
BNO-DPAC	450	30	15.2	(0.155, 0.068)	14
NBO-pSAF	451	26	20.5	(0.147, 0.048)	15
IDCzBNO	460	28	11.5	(0.14, 0.08)	16
2B-DTACrs	447	26	14.8	(0.150, 0.044)	17
BOBO-Z	445	18	13.6	(0.15, 0.04)	
BOBS-Z	456	23	26.9	(0.14, 0.06)	18
BSBS-Z	463	22	26.8	(0.13, 0.08)	
NOBNacene	412	41	8.5	(0.173, 0.055)	19
MesB-DIDOBNA-N	402	22	9.3	(0.165, 0.044)	20
TPD4PA	455	29	30.7	(0.14, 0.06)	21
tBu-TPD4PA	460	29	32.5	(0.14, 0.07)	
DBCz-Mes	451	16	16.2	(0.147, 0.038)	22
DBCz-Mes*	452	17	33.9	(0.144, 0.058)	
f-DOABNA	445	24	19.9	(0.150, 0.041)	23
DOB2-DABNA-A	452	24	24.1	(0.145, 0.049).	24
DPA-B2	444	31	28.9	(0.153, 0.055)	
DPA-B3	450	15	37.7	(0.150, 0.043)	25
DPA-B4	457	14	39.2	(0.141, 0.050)	
Cz-B4	457	26	32.1	(0.138, 0.076)	

Py-BN	444	21	15.8	(0.153, 0.045)	
Py-BN*	445	22	27.7	(0.150, 0.052)	26
Pm-BN	415	24	5.8	(0.161, 0.045)	
BIC-mCz*	432	42	19.4	(0.16, 0.05)	27
mDBIC*	431	42	13.5	(0.16, 0.05)	
BN1*	457	28	31.2	(0.14, 0.08)	28
BN3*	458	23	37.6	(0.14, 0.08)	

\* Ternary OLEDs with sensitizers.



**Fig. S11.** The molecular structure of m4TCzPhBN and UV–vis absorption of c-DABNA and emission spectra of m4TCzPhBN in dilute toluene solution.



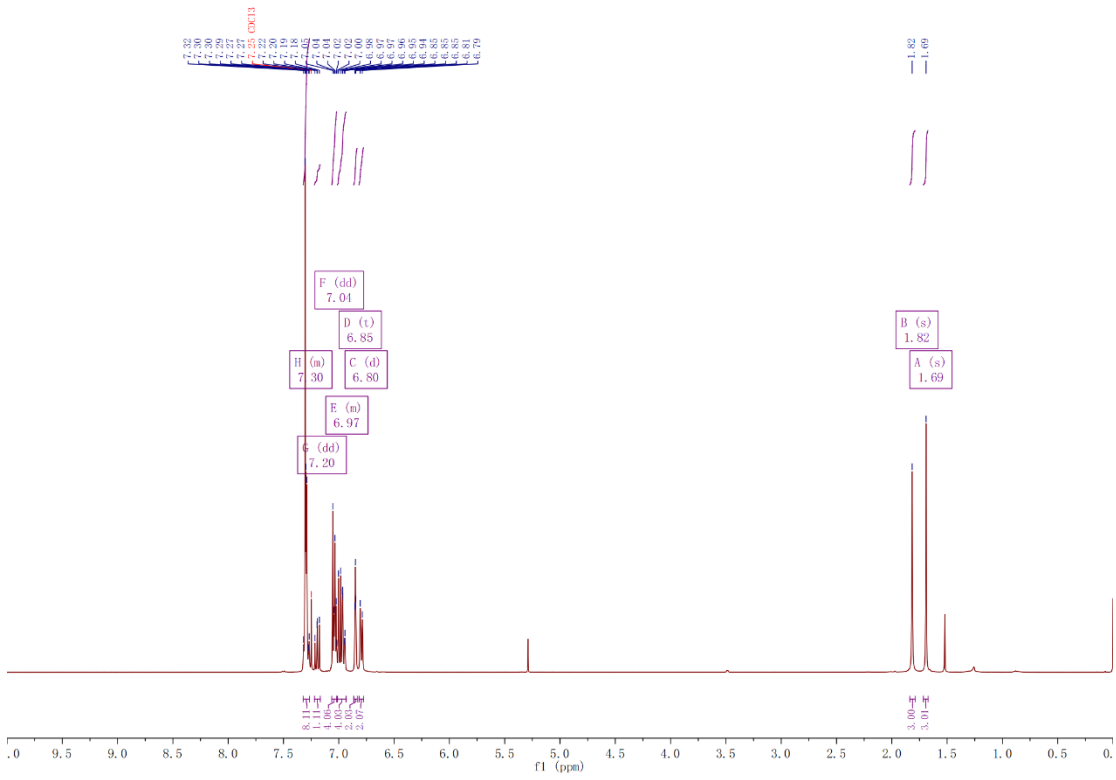


**Fig. S14.**  $^1\text{H}$  NMR spectrum of intermediate **2** in  $\text{CDCl}_3$ .

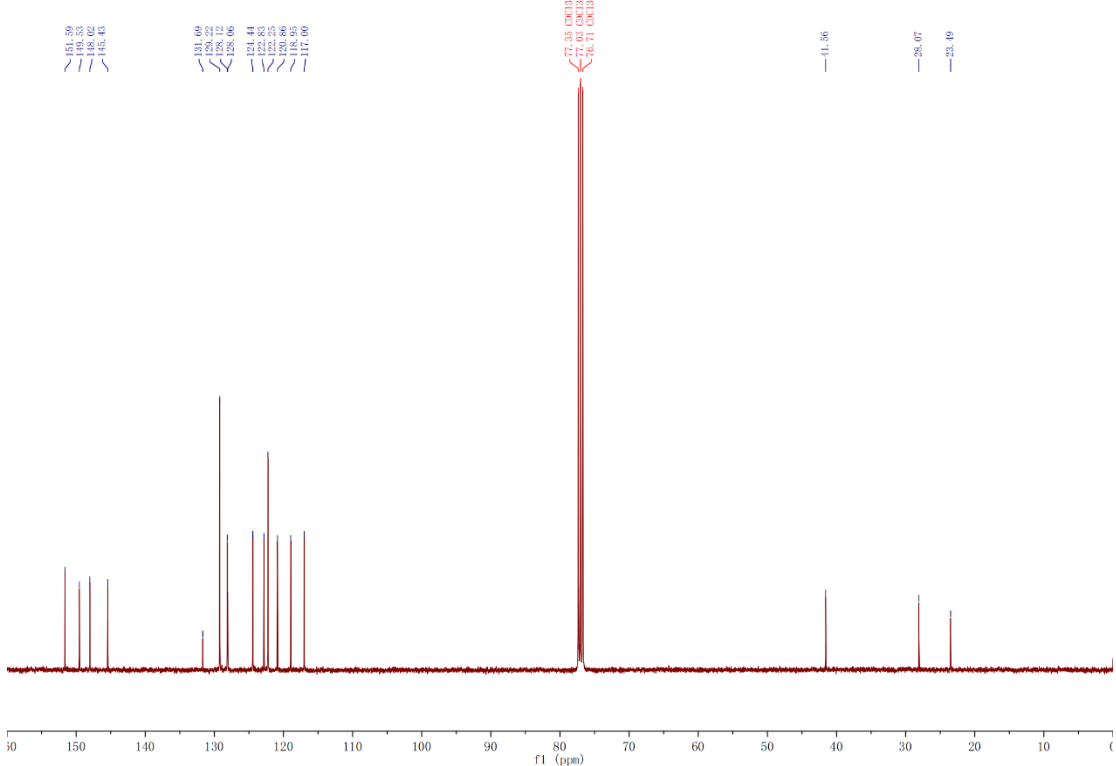


**Fig. S15.**  $^{13}\text{C}$  NMR spectrum of intermediate **2** in  $\text{CDCl}_3$ .

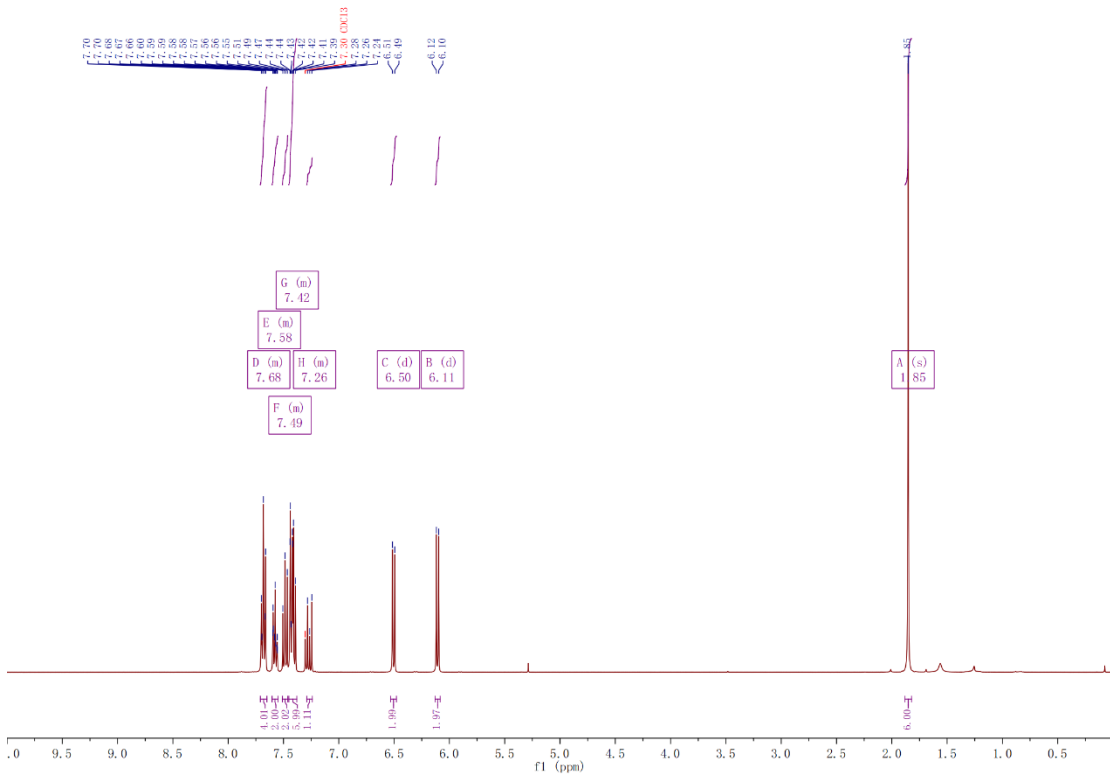


**Fig. S16.**  $^1\text{H}$  NMR spectrum of c-DABNA in  $\text{CDCl}_3$ .

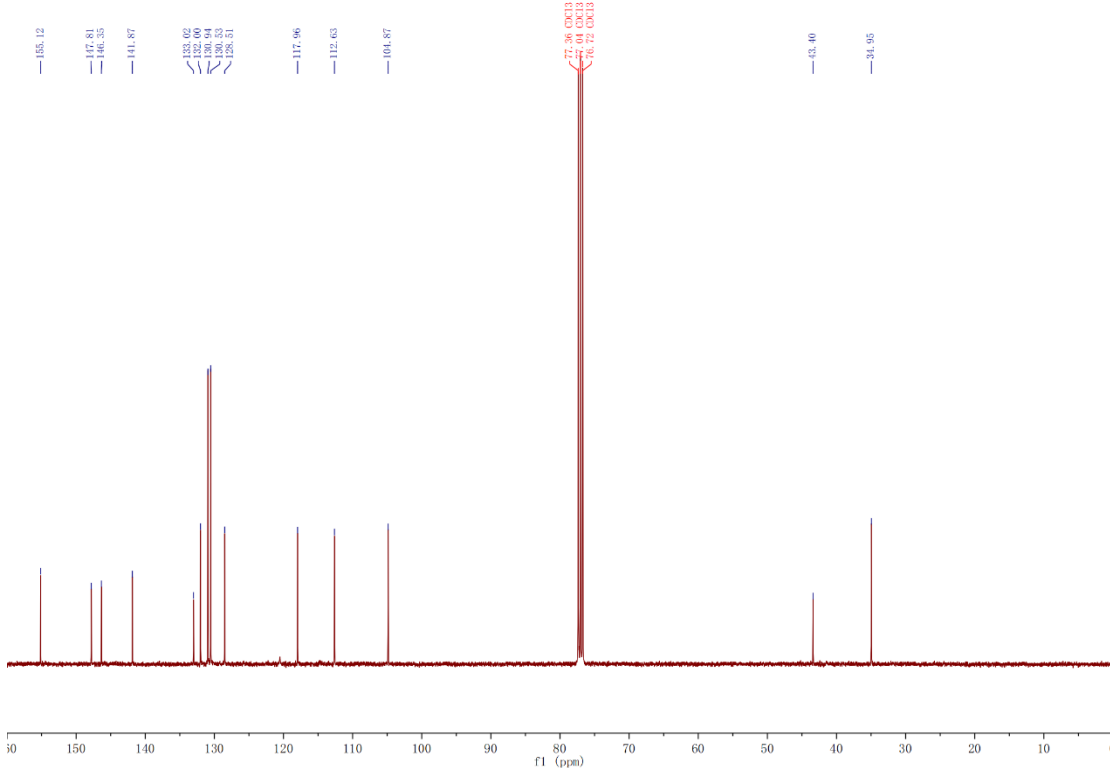


**Fig. S17.**  $^{13}\text{C}$  NMR spectrum of c-DABNA in  $\text{CDCl}_3$ .

## Reference

- 1 T. Lu, F. W. Chen, *J. Comput. Chem.* **2012**, *33*, 580.
- 2 W. Humphrey, A. Dalke, K. Schulten, *J. Mol. Graph.* **1996**, *14*, 33.
- 3 Y. X. Wang, Y. L. Duan, R. D. Guo, S. F. Ye, K. Y. Di, W. Z. Zhang, S. Q. Zhuang, L. Wang, *Org. Electron.* **2021**, *97*, 106275.
- 4 M. X. Xing, G. H. Chen, S. N. Wang, X. J. Yin, J. H. Liu, Z. X. Xue, N. Q. Li, J. S. Miao, Z. Y. Huang, C. L. Yang, *Adv. Funct. Mater.* **2024**, 2414635.
- 5 X. F. Song, S. Luo, N. Q. Li, X. T. Wan, J. S. Miao, Y. Zou, K. Li, C. L. Yang, *Angew. Chem. Int. Ed.* **2025**, *64*, e202413536.
- 6 D. R. Wan, J. P. Zhou, Y. Yang, G. Y. Meng, D. D. Zhang, L. Duan, J. Q. Ding, *Adv. Mater.* **2024**, *36*, 2409706.
- 7 B. X. Li, J. L. Lou, B. J. Zhang, L. Liu, X. He, H. Xu, X. Feng, H. Zhang, Z. M. Wang, B. Z. Tang, *Chem. Eng. J.* **2024**, *482*, 148876.
- 8 K. R. Naveen, H. Lee, R. Braveenth, K. J. Yang, S. J. Hwang, J. H. Kwon, *Chem. Eng. J.* **2022**, *432*, 134381.
- 9 M. Mamada, A. Aoyama, R. Uchida, J. Ochi, S. Oda, Y. Kondo, M. Kondo, T. Hatakeyama, *Adv. Mater.* **2024**, *36*, 2402905.
- 10 T. J. Fan, Y. W. Zhang, L. Wang, Q. Wang, C. Yin, M. X. Du, X. Q. Jia, G. M. Li, L. Duan, *Angew. Chem. Int. Ed.* **2022**, *61*, e202213585.
- 11 J. Park, J. Lim, J. H. Lee, B. Jang, J. H. Han, S. S. Yoon, J. Y. Lee, *ACS Appl. Mater. Interfaces* **2021**, *13*, 45798.
- 12 J. M. Han, Z. Y. Huang, X. Lv, J. S. Miao, Y. T. Qiu, X. S. Cao, C. L. Yang, *Adv. Opt. Mater.* **2022**, *10*, 2102092.
- 13 I. S. Park, H. Min, T. Yasuda, *Angew. Chem. Int. Ed.* **2022**, *61*, e202205684.
- 14 X. Y. Huang, Y. L. Xu, J. S. Miao, Y. Y. Jing, S. N. Wang, Z. Y. Ye, Z. Y. Huang, X. S. Cao, C. L. Yang, *J. Mater. Chem. C* **2023**, *11*, 11885.
- 15 J. Jin, Z. L. He, D. Liu, Y. Q. Mei, J. H. Wang, H. H. Wan, J. Y. Li, *Chem. Sci.* **2024**, *15*, 18135.
- 16 T. J. Fan, Q. W. Liu, L. Duan, D. D. Zhang, *J. Mater. Chem. C* **2024**, *12*, 7989.
- 17 C. Y. Chan, S. M. Suresh, Y. T. Lee, Y. Tsuchiya, T. Matulaitis, D. Hall, A. M. Z. Slawin, S. Warriner, D. Beljonne, Y. Olivier, C. Adachi, E. Zysman-Colman, *Chem. Commun.* **2022**, *58*, 9377.
- 18 I. S. Park, M. L. Yang, H. Shibata, N. Amanokura, T. Yasuda, *Adv. Mater.* **2022**, *34*, e202107951.
- 19 S. M. Suresh, L. Zhang, D. Hall, C. F. Si, G. Ricci, T. Matulaitis, A. M. Z. Slawin, S. Warriner, Y. Olivier, I. D. W. Samuel, E. Zysman-Colman, *Angew. Chem. Int. Ed.* **2023**, *62*, e202215522.
- 20 S. M. Suresh, L. Zhang, T. Matulaitis, D. Hall, C. F. Si, G. Ricci, A. M. Z. Slawin, S. Warriner, D. Beljonne, Y. Olivier, I. D. W. Samuel, E. Zysman-Colman, *Adv. Mater.* **2023**, *35*, 2300997.
- 21 K. R. Naveen, H. Y. A. Lee, L. H. Seung, Y. H. Jung, C. P. K. Prabhu, S. Muruganantham, J. H. Kwon, *Chem. Eng. J.* **2023**, *451*, 138498.
- 22 X. Wang, L. Wang, G. Y. Meng, X. Zeng, D. D. Zhang, L. Duan, *Sci. Adv.* **2023**, *9*, adh1434.
- 23 R. W. Weerasinghe, S. M. Suresh, D. Hall, T. Matulaitis, A. M. Z. Slawin, S. Warriner, Y. T. Lee, C. Y. Chan, Y. Tsuchiya, E. Zysman-Colman, C. Adachi, *Adv. Mater.* **2024**, *36*, 2402289.
- 24 J. Ochi, Y. Yamasaki, K. Tanaka, Y. Kondo, K. Isayama, S. Oda, M. Kondo, T. Hatakeyama, *Nat. Commun.* **2024**, *15*, 2361.
- 25 T. Hua, X. S. Cao, J. S. Miao, X. J. Yin, Z. X. Chen, Z. Y. Huang, C. L. Yang, *Nat. Photonics* **2024**, *18*, 1161.
- 26 X. L. Cai, Y. Pan, C. L. Li, L. J. Li, Y. X. Pu, Y. W. Wu, Y. Wang, *Angew. Chem. Int. Ed.* **2024**, *63*, e202408522.
- 27 X. Wang, Y. W. Zhang, H. Y. Dai, G. M. Li, M. H. Liu, G. Y. Meng, X. Zeng, T. Y. Huang, L. Wang, Q. Peng, D. Z. Yang, D. G. Ma, D. D. Zhang, L. Duan, *Angew. Chem. Int. Ed.* **2022**, *61*, e202206916.
- 28 X. L. Lv, J. S. Miao, M. H. Liu, Q. Peng, C. Zhong, Y. X. Hu, X. S. Cao, H. Wu, Y. Y. Yang, C. J. Zhou, J. Z. Ma, Y. Zou, C. L. Yang, *Angew. Chem. Int. Ed.* **2022**, *61*, e202201588.